## Advanced Journal of Engineering and Scientific Applications (AJESA)

Research Paper Open Access

Available online at www.ajesa.com.ng

Vol. 2 No.1, 2025. pp.59-73



# Experimental Investigation of High Filler Loading of SiO<sub>2</sub> on the Mechanical and Dynamic Mechanical Analysis of Natural PALF fibre-Based Hybrid Composite

## George O. Okoronkwo<sup>1</sup>, Ibe Kizito Chidozie<sup>2</sup>, Faloye Mayowa Emmanuel<sup>3</sup>

<sup>1</sup>Department of Chemical Engineering, Micheal Okpara University of Agriculture, Umudike, Abia State, Nigeria; okoronkwo.george@mouau.edu.ng, ogeorgeonyeka@gmail.com

<sup>2</sup>Department of Civil Engineering, Micheal Okpara University of Agriculture, Umudike, Abia State, Nigeria ibe.kizito@mouau.edu.ng

Corresponding Author::ogeorgeonyeka@gmail.com

#### Abstract

This work aims to experimentally investigate high filler loading of on the mechanical and dynamic mechanical analysis of natural PALF fibre-based hybrid composite. The compression moulding process was used to fabricate the composite. To achieve the aforementioned goals, the blends were made using 25 % PALF and varied weight proportions (3wt. %, 6wt. %, and 9 wt. %) of nanoparticles. Tensile, bending, impact, interlaminar shear, shoreline D hardness, and dynamic mechanical analysis were all evaluated. SEM was used to examine the morphology of the materials, and an FTIR spectrometer was used to look for the presence of organic chemicals in fiber-reinforced composite materials. The findings show that adding 25 % PALF fiber and 6 % nanoparticles (D-type) to the epoxy polymer improved the thermal and mechanical properties of the composites. It can be attributed to the improved interaction and homogeneous dispersion of the fillers and epoxy polymers. Moreover, the water uptake parameters of all samples were studied. The findings showed that the inclusion of reinforcements boosts the water uptake of the composite significantly. The initial deterioration rate of the -incorporated hybrids is almost the same, at about 400°C, which is considerably greater than that of the beginning breakdown temperatures of PALF (300°C), according to the thermography study. This might imply that the fiber and polymers form a stronger bond, reducing polymer movement and increasing the thermo-stability of the combination.

KEYWORDS: PALF fiber, , Mechanical properties, Dynamic Analysis, FTIR, Water absorption

#### 1. INTRODUCTION

In the current context, there is a growing desire for innovative composite materials with increased properties to meet distinct performance needs (Okoronkwo et al. 2022). The general approach for developing substances is the introduction of fillers and ber reinforcements to plastics. Polymers have expanded their possible applications in so many organizations due to their high resistance to corrosion, low price, and lightweight. Epoxy polymers have superior mechanical properties, good dimensional durability, and better heat resistance than other thermoplastic and thermoset polymers. Furthermore, when epoxy resins go through the hardening process, they become fragile. Brittleness is an indication of a serious problem that can be mitigated by the use of artificial filler or organic fiber ((Gholampour et al.2020); (Väisänen et al. 2017)). The enormous accomplishment of sturdy synthetic and natural

<sup>&</sup>lt;sup>3</sup>Department of Civil Engineering, Micheal Okpara University of Agriculture, Umudike, Abia State, Nigeria faloyemayow@gmail.com

cloth merged in plastic is acknowledged and anchored. Nevertheless, these constant fiber-based polymeric plastic laminates have some disadvantages, such as debonding, which can be avoided by using nano or micro fillers instead of long fibers. Such constraints often constrain its application area and create a need for polymer plastic laminate to improve. Furthermore, significant growing worries and awareness of an eco-friendly and better ecosystem in society sharpened a deep belief in natural fiber and filler (Velmurugan et al. 2020). The use of various environmentally friendly and recyclable reinforcing materials, for example, leaves of plants, cotton, jute, wood powder, coir dust, axseed, wheat, grain, and so on, are encouraged. Rather than different efforts towards employing environmentally friendly and renewable polymers for commercial processes, a key disadvantage has been found in the thermomechanical properties. In recent years, the majority of polymer laminates were created using arti cial and organic textiles ((Sharma et al.2020); (Gouda et al. 2021); (Sanjay et al. 2018)). Of all regularly utilized biological fibers, pineapple leaf (PALF) fibers possess the greatest promise for usage as reinforcing in ber or powdered format to create a high-tensile, inexpensive, and recyclable biocompatible product. PALF fibers are multilayer fibers derived from pineapple leaves (Johny et al. 2023). PALF fibers are preferred over other natural fabrics due to their high cellulose content (70-85%), which leads to higher bending and tensile qualities than axseed, jute, sisal, and wool fibers. PALF has similar bending and twisting stiffness to jute fiber. PALF is widely available, has a low density, a good aspect ratio, as well as a small microbrillar inclination (Johny et al. 2023). (Ponnusamy et al. 2022) observed that PALF does have a high modulus and has a great potential for usage in the chemical industries. According to (Natrayan et al. 2022) the exposure to 30 phr PALF raised the compressive and tearing strengths of NBR laminate to 15 psi and 200 kN/mm, respectively. According to (Ponnusamy et al. 2022) the PALF may be efficiently employed in a polypropylene matrix. Despite a wide range of favorable qualities, PALF has lower impact strength than rice husk. To increase their qualities holistically, PALF as well as other fibers or fillers must be reinforced within a single polymer matrix. The combination of a rigid and moderately elastic fiber with an extreme load-to-failure fiber increases the fracture toughness of the resultant composite (Todkar et al. 2019). Furthermore, combining one kind of organic fiber with the other gives a noteworthy and workable option that leads to multipurpose composites having great creep and wear strength and better impact strength (G V et al. 2020). For instance, polymers with silicon dioxide (SiO<sub>2</sub>) nanoparticles have outstanding physical, thermodynamic, as well as other characteristics. It should be noted that SiO2 nanoparticles are currently being investigated as potential replacements in polymeric matrices. (Lakshmaiya et al. 2022) conducted tensile and fracturing experiments using scattered silicon in an epoxy coating, finding that the inclusion of 5% nano llers might increase rigidity and breakage energies. Nano-SiO<sub>2</sub> is an ecologically friendly product with a composition comparable to basalt fiber. Due to its rich content, excellent eficiency, extensive surface area, tiny sizes, and high adsorption, it is extensively used in coatings, polymers, and chemicals, as well as other industries. (Natrayan et al. 2022) covered sandblasting iron using composite material made of micro- and nano- SiO<sub>2</sub> particles as well as an epoxy polymeric foundation, accordingly. In a saline spraying test, the composites were weathered. According to studies, nano- SiO<sub>2</sub> coatings are more corrosion-resistant than micro- SiO<sub>2</sub> coatings (Velmurugan et al. 2023). When compared to conventional epoxy coating, the impact resistance of hardened epoxy coating increased from 0.71 MPa to 0.93 MPa, a 20.2% rise, as well as the glass transition point from 200 °C to 158 °C, implying that nano-SiO<sub>2</sub> incorporation dramatically improved the damage tolerance and elevated heat resistance of the epoxy coating (Velmurugan et al. 2022). Several researchers have treated the surfaces of fibers with nano-SiO<sub>2</sub>. (Maurya et al. 2022) used a sol-gel approach to transplant a SiO<sub>2</sub> covering with such a nano porosity architecture on the surfaces of PBO fibers. The adhesion strength among the altered PBO/SiO2 fiber and epoxy was discovered to be dramatically improved, the interface's shear force rose by 123.25%, and the hydrophobic nature also was highly improved. (Tang et al. 2017) created an aramid fiber insulation sheet by processing this with 1 wt. % of SiO<sub>2</sub>. Both mechanical and electrical testing was performed on the aramid fiber insulation sheet before and following modifications. A significant interfacial impact between nano-SiO2 and synthetic fibers was discovered, resulting in a 1% improvement in tensile strength, deformation at breaking, and dielectric breakdown power (Ponnusamy et al. 2022). As contrasted to untreated aramid insulation sheets, SiO<sub>2</sub>-modi ed aramid fiber insulation paper improved by 7.5%, 10%, and 14%, respectively. The physical and dielectric characteristics of a carbon ber insulation sheet were enhanced as a result. Cheng et al. found that increasing the silica concentration improved the compression strength of glass-epoxy hybrids (Chai et al. 2022). The improved strength of concrete might be ascribed to improved interfacial adhesion caused by the scattered silica nanoparticles. Admittedly, few research projects have focused on the effect of laminate architectures as well as the role of inorganic nanoparticles such as SiO<sub>2</sub> particles on the characteristics of PALF composite materials based on epoxy. The purpose of this work was to establish the possibility of producing PALF/SiO2-based hybrid materials with varying filler weight proportions. To achieve the aforementioned goals, the mechanical and dynamic mechanical characteristics of the composites were investigated.

#### 2. MATERIALS AND METHODS

#### 2.1 Materials

#### 2.1 Materials

In this investigation, artificial epoxy resin YD-535 LV as well as curing agent TH-725 were obtained from the C.K. pharmaceutical sector and employed as polymer matrices. PALF fibers acquired at Salam, Tamil Nadu, India, were used as reinforcing material in the production of synthetic epoxy composites. In this study, synthetic fillers such as SiO<sub>2</sub> (10 nm in particle size) were used. Figure 1 depicts photographs of reinforcements and fillers. Before using the PALF fiber its thoroughly washed with clean water and then treated with alkaline and silane solutions to enhance the interfacial bonding.



Figure 1. Photographic Images of (a) PALF fiber, (b) SiO<sub>2</sub> nanoparticles

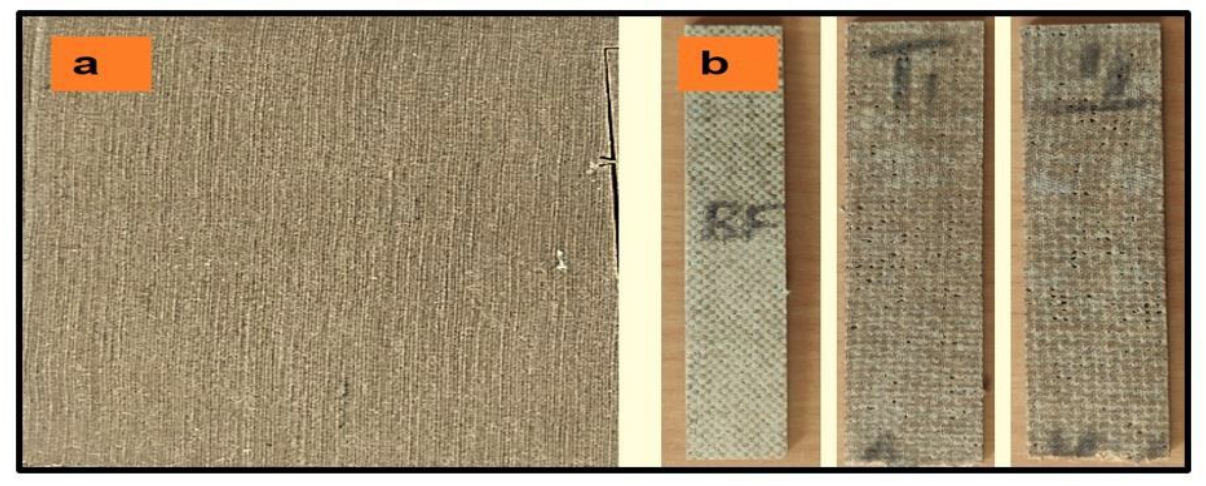


Figure 2. Fabricated composites of (a) Overall Plate, (b) Test specimen

### 2.2 Fabrication of Composite Laminate

The purchased PALF fibers were cleansed with running, pure tap water to wash away dirt and other foreign elements before being dried in the sunlight for 70 hours to eliminate any remaining wetness. The PALF fibers are chopped into little pieces and fed into standard slicing milling equipment to generate micro-particles of PALF fibers, which are then sieved through a 250-mesh screen. To use an electronic weight device, the epoxy polymers, curing agent, and reinforcing components were accurately weighed in varied weight proportions. The weight percentage for the manufacture of epoxy composite samples from PALF fiber and SiO<sub>2</sub> nanoparticles is shown in Table 1. Mechanical stirring was utilized to achieve homogeneous particulate distribution inside the resin. To prevent sudden drying, the combined liquid was promptly transferred to the mould and permitted to drain for real curing. To lower the interior water content, the created sample was poured into the mould and transported to the burner, which was set to 70°C (after drying). Figure 2 shows the image of fabricated and tested composite samples.



© 2025. Advanced Journal of Engineering and Scientific Applications (AJESA) Vol. 2, No..1, 2025.

Table 1 Composite Fabrication based on the weight ratios of fiber/ fillers

Sl.	Sample	Sample	Weight %	Weight Ratio	Weight %
No	Symbol	Descriptions	of Epoxy resin	of PALF	of SiO <sub>2</sub>
1	A	Pure Epoxy	100	-	-
2	В	Epoxy/PALF	75	25	_
3	C	Epoxy/PALF/SiO <sub>2</sub>	72	25	3
4	D	Epoxy/PALF/SiO <sub>2</sub>	69	25	6
5	E	Epoxy/PALF/SiO <sub>2</sub>	66	25	9

#### 2.3 Composite Fabrication

These involve:

#### 2.3.1 Mechanical Properties

Tensile testing was carried out to measure the tensile strength of a manufactured epoxy-based polymeric hybrid composite. By the ASTM D 3039 standards, the sample was made into a rectangle with measurements of 25 mm in width, 250 mm in length, and 3 mm in thickness. This study was carried out at a crosshead velocity of 1 mm/min until the breakage was achieved. The three-point bending specimen was generated in Comtech's universal tester by the ASTM D790 standards for three-point bending tests. The deformation of an epoxy-based hybrid composite during compressive stresses was determined until the sample broke or cracked. All experimental materials had their bending movement and loading evaluated by the apparatus. The dimensions of the reinforced epoxy laminate sample for this study are 12.7 mm wide, 128 mm long, and 3 mm thick. The ASTM D2344-84 standards were employed to evaluate the fracture characteristics of polymers using interlaminar testing. Sections of epoxy composite samples were cut at 18 mm in length, 6 mm in width, and 3 mm in thickness. The assessment includes a spanning length of thirty mm and a speed of one millimeter per minute. The fracture toughness of epoxy polymeric composites is defined as their ability to absorb power from such an impact force in the context of a smooth surface that centers on strains. The izod impact test was carried out by the ASTM D 256 standards. Deformation durability testing equipment was used to assess the Shore D hardness of epoxy polymeric composites. An indenter was pushed against the reinforced hybrid composite sample until the bottom section of the indenter made total contact with the lamination. The polymeric characteristics can affect' hardness, which is indicated using the hardness indenter. The experiment was carried out at three different spots on the lamination, and the mean toughness was computed.

#### 2.3.2 Thermal Stability

TGA testing was performed on epoxy hybrid composites in a nitrogen environment at temperatures ranging from 30 to 800°C. Utilizing derivative thermal images, weight loss was evaluated, and leftover charcoal concentration was investigated at 700 °C. The scanning electron microscopy technique was used to examine the surface structure of a hybrid composite. Before this, all of the specimens were covered with auricular dust. The hybridization interaction among the PALF ber matrix and SiO<sub>2</sub> nanoparticles was shown using Fourier transform infrared spectroscopy.

#### 2.3.3 Moisture Absorption

The water uptake research for epoxy composite materials was performed by the ASTM D 570 specification. The specimen was dried in a furnace for a specific period at a specific temperature (60°C), and its original weight was determined. The resulting epoxy-hybrid materials were then submerged in water for 60 days at ambient temperature. Following immersion, specimens were retrieved, extra water was wiped away using a towel, and they were measured again. The difference in weights between the beginning and final weights was recorded.

#### 3. RESULTS AND DISCUSSION

#### 3.1 FTIR characterization

The existence of organic compounds in fiber-reinforced epoxy composites was investigated using an FTIR spectrometer. The substituents of a composite's constituents were determined using FTIR. This substituent was identified using the FTIR attenuated whole reflection (ATR) equipment. The wavelength spectrum of the equipment was  $500-4000~\rm cm^{-1}$ . The transparency setting was used to capture the FTIR spectrum. Figure 3 depicts the FTIR spectroscopy of the PALF composite. An O-H group's feature was noticeable among the intensities of 3200 and 3550 cm<sup>-1</sup>. Peaks for C-H extending and C=O extending are located at  $2801-2850~\rm cm^{-1}$  and  $1601-1650~\rm cm^{-1}$ , respectively. The wavelength region  $1200-1300~\rm cm^{-1}$  in the Figure 3 reveals C-H binding. The spectral analysis of PALF ber had changed following hybridization with SiO<sub>2</sub> nanoparticles. The bending vibration of N-H groupings



© 2025. Advanced Journal of Engineering and Scientific Applications (AJESA) Vol. 2, No..1, 2025.

around 2800 cm<sup>-1</sup> was widened, perhaps due to interactions of hydrogen bonds among SiO2 nanoparticles and PALF fiber (Kavya et al. 2021). Trend shifts from 1793 to 1798 cm<sup>-1</sup> as well as 3640 to 3680 cm<sup>-1</sup>, correspondingly, guarantee the presence of the hydroxyl group among -OH and -C = O. The vibrating wavelength of Si-OH changes from 3923 to 3969 cm<sup>-1</sup>, indicating the presence of silicon in the epoxy. It was possible to determine that there were substantial contacts between the SiO<sub>2</sub> nanoparticles and the PALF fiber. So, these contacts might be diverse, including the previously stated hydrogen atoms and cytotoxic processes, in addition to electrostatic attraction among SiO<sub>2</sub> nanoparticles and PALF fiber (Hoque et al. 2018).

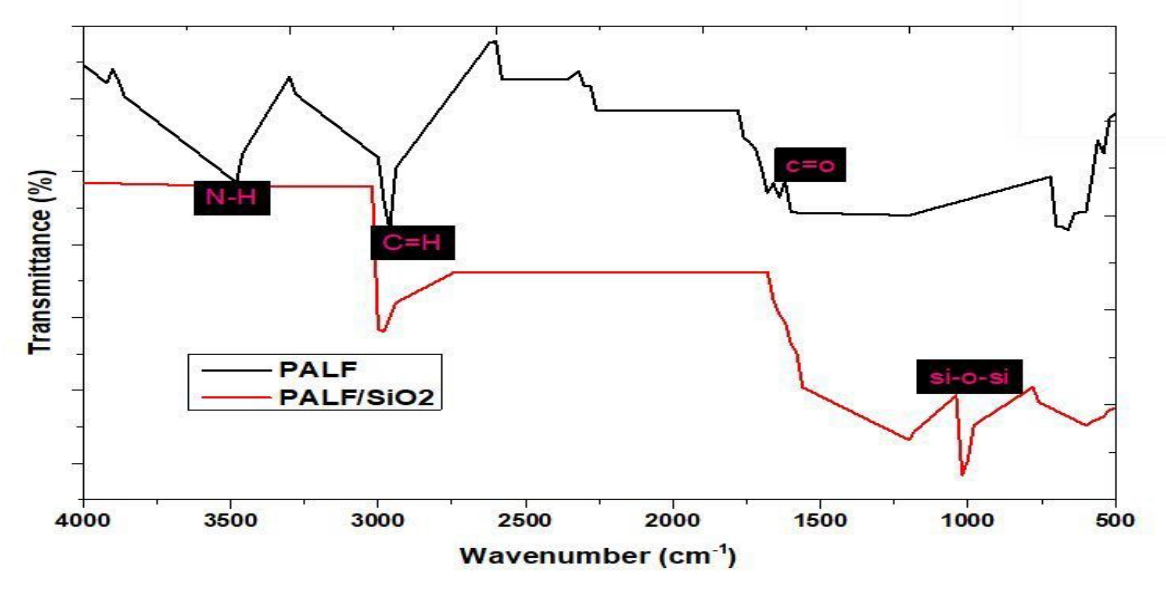


Figure 3. FTIR analysis of PALF and PALF/  ${\rm SiO_2}$  based hybrid composites

#### 3.2 Mechanical Properties

These are:

#### 3.2.1 Tensile behavior

Many studies have shown that strengthening polymeric materials with such a low weight percentage of ller materials and natural materials yields the best mechanical characteristics. The cited comment has been in favor of D-type specimens. It was anticipated that combining a 6 wt. % SiO<sub>2</sub> composite with natural fiber would improve the mechanical characteristics of hybrid composites. As shown in Figure 4, each of the hybrid composites (C-type, D-type, and E-type) had higher tensile strength and modulus than the A and B-type. Even though contrasted with pure resin, hybrids laminate C, D, and E-type demonstrated 13.25 %, 23.369 %, and 20.36 % increases in tensile strength as well as 32.65 %, 45.62 %, and 40.12 % increases in elastic strength. This improvement in both modulus and tensile strength was made feasible by the hybrid composite's proper dispersion of 6 wt. % SiO<sub>2</sub>, which facilitated efficient load transmission, as reported earlier by investigators (Natrayan et al. 2018). Moreover, the high adhesiveness of the alkalisilane-modified PALF fiber as well as the epoxy composite results in excellent binding at its contact point. Esters, hydrophobic interactions, and copolymer (NH-CO) production might occur during the metaphase between the PALF fiber and the basic matrices. Its collective effects of the nano-SiO<sub>2</sub> fillers and processed PALF fiber guarantee that the combination has good strength. As a result, for the previously indicated scenario, significant hybridization is being found. The tensile strength of the composites decreased as the SiO<sub>2</sub> concentration increased (over 6 wt. %). This is really due to the build-up of ller particles in the epoxy. This might be because SiO<sub>2</sub> nanoparticles accumulated on the fiber surface and caused numerous flaws, like fractures. Once the tension load was applied to the fiber, the fractures spread widely and spread from the handling to the fiber surface, leading to several maximum stress points on that surface and speeding fiber breakage.

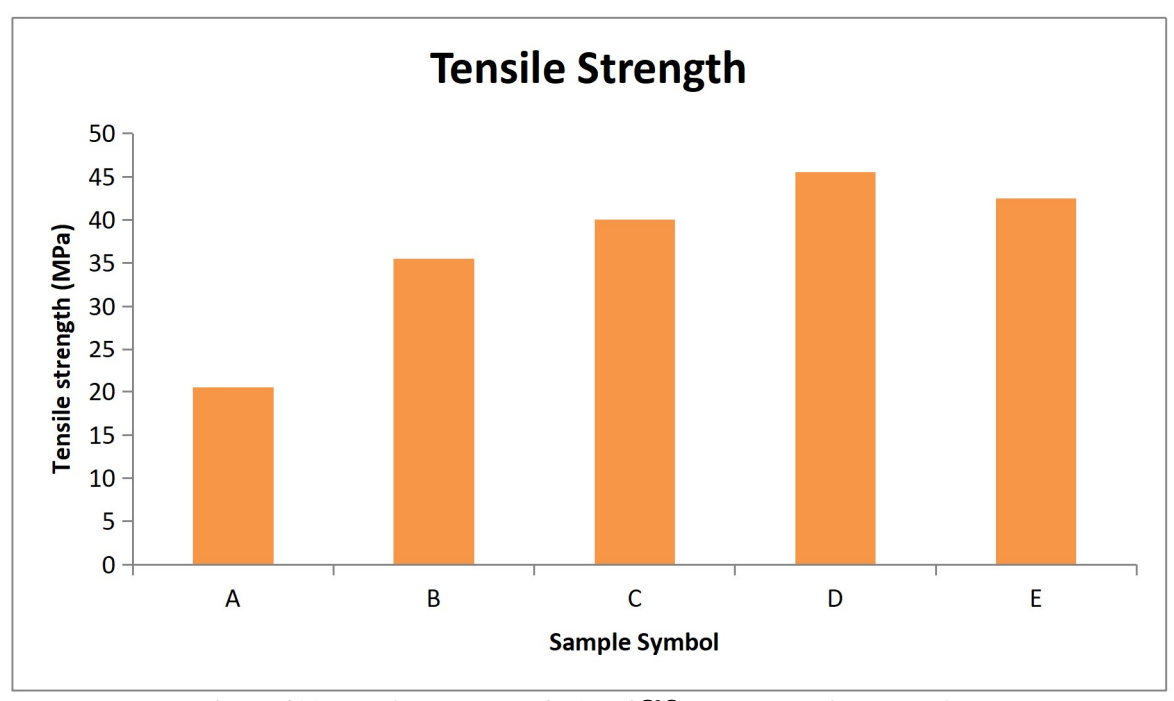


Figure 4(a). Tensile strength of PALF/SiO<sub>2</sub>-based hybrid composites

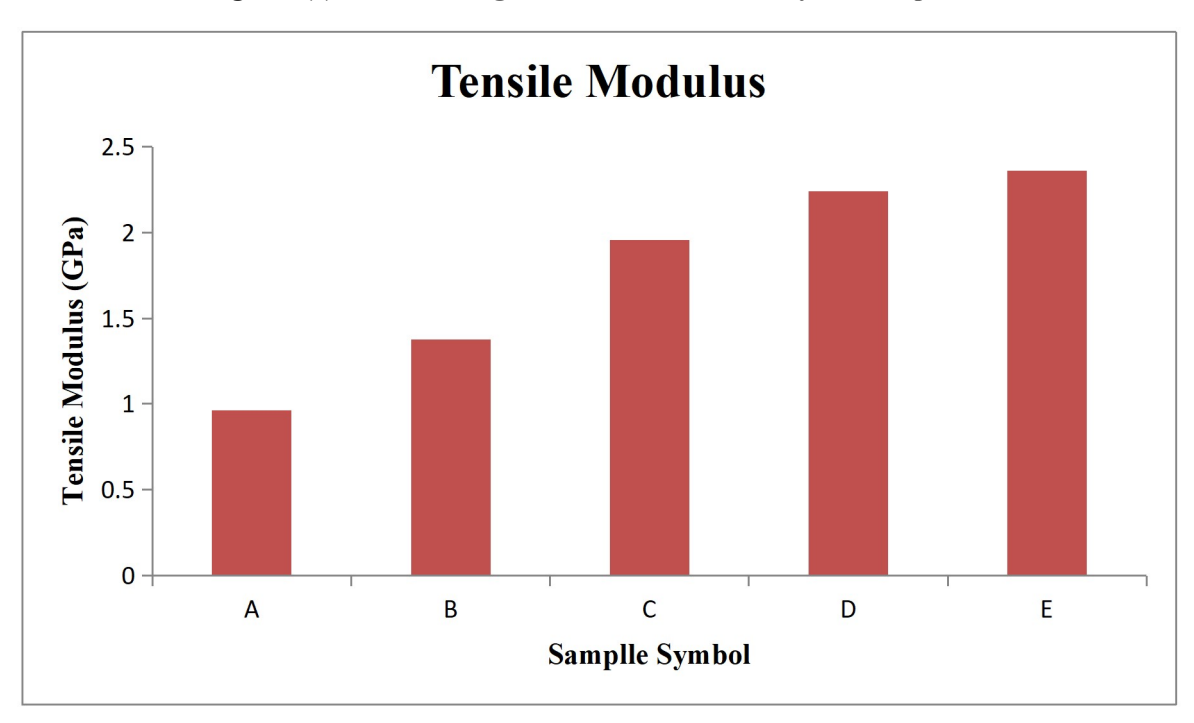


Figure 4(b). Tensile Modulus of PALF/SiO<sub>2</sub>-based hybrid composites

#### 3.2.2 Flexural Behaviour

Figure 5 depicts the flexural behavior of epoxy as well as all-hybrid composites. Surprisingly, all of the materials show the same trend for bending modulus and strength as they do for tension characteristics. Flexural characteristics of PALF/SiO<sub>2</sub>-derived hybrid materials C, D, and E are greatly enhanced as compared to regular epoxy. The bending strengths rose by 30 %, 42 %, and 45 % in bio-composites such as C-type, D-type, and E-type, respectively. This increase was caused by the efficient load transfer across matrices to reinforcements as a consequence of the strong esters, hydroxyls, and nylon binding interactions among PALF fiber and resin, as well as the good distribution of nanocrystalline silicon dioxide. It had also been predicted that nano SiO<sub>2</sub> would have minimized the gap between the strengthening PALF fiber and matrix. This finding is in contrast with (Hamid et al. 2019). The E-type of all materials had the maximum flexural strength (58.96 MPa) and elasticity (2.79 GPa), whereas the A-type had the least strength properties at 26.32 MPa and elasticity of 0.85 GPA. Tensile property trends were also detected for flexural characteristics, indicating a favorable hybridized impact. A high adhesion/interaction between the PALF fiber and



© 2025. Advanced Journal of Engineering and Scientific Applications (AJESA) Vol. 2, No..1, 2025.

epoxy contact, as well as the addition of nanocrystalline SiO<sub>2</sub>, results in improved load transmission. Furthermore, as previously reported, superior SiO<sub>2</sub> dispersal and distance decrease among PALF ber and epoxy matrices contacts should have had an important impact in boosting load transmission from matrices to PALF fiber.

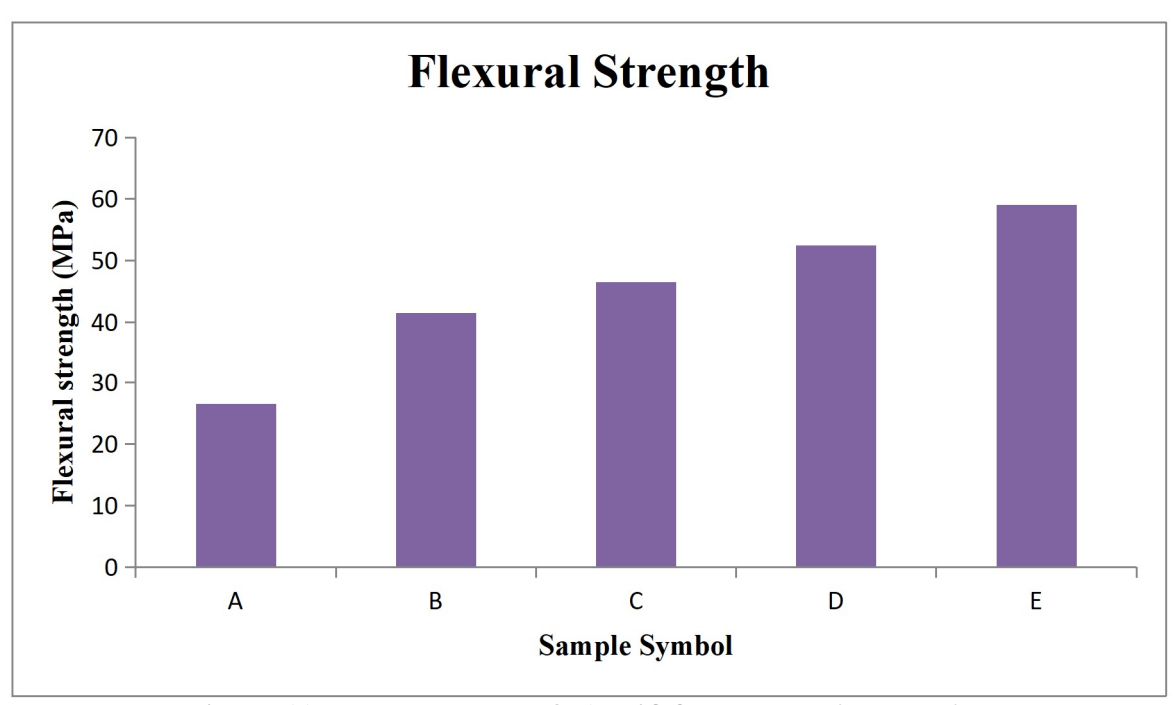


Figure 5(a): Flexural strength of PALF/SiO<sub>2</sub>-based hybrid composites

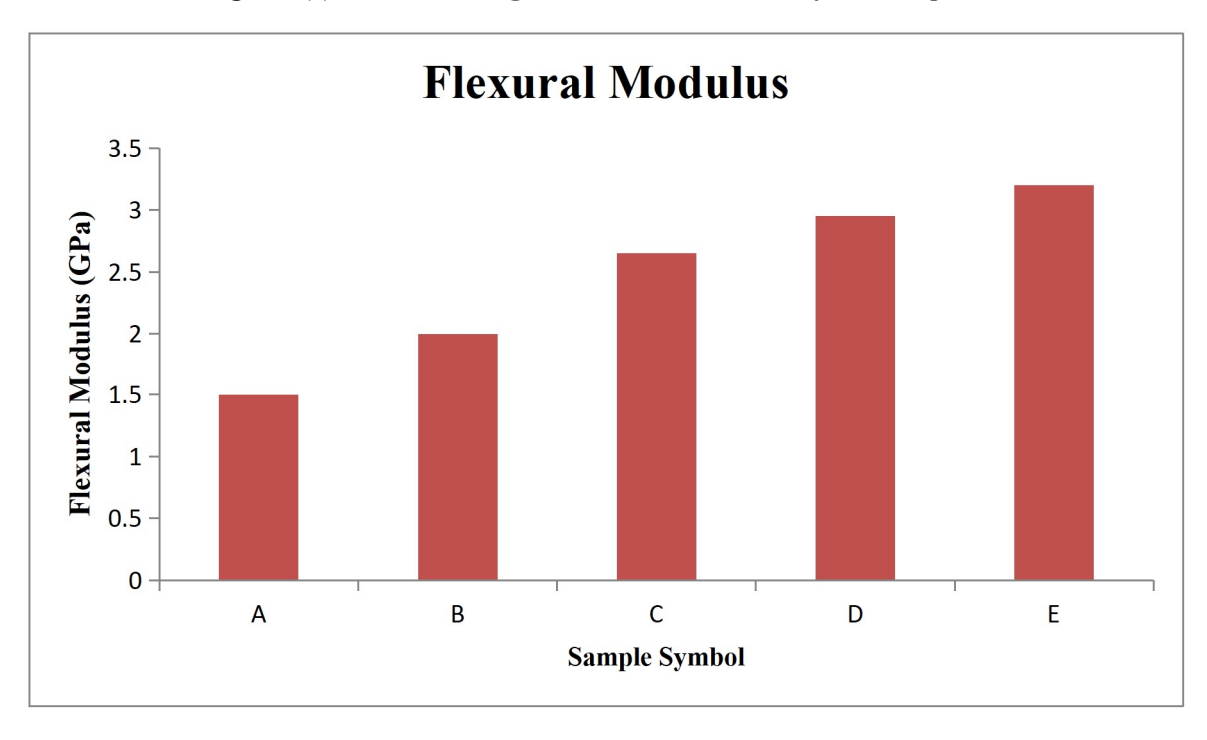


Figure 5(b): Flexural Modulus of PALF/SiO<sub>2</sub>-based hybrid composites

#### 3.2.3 Interlaminar Shear strength

For instance, the interlaminar shear of an elastomeric polymeric matrix is vulnerable to the formation of voids and interfacial adhesion between the filler and the polymers. The produced composites were tested for resistance against inter-laminar strength properties. Figure 6 depicts the inter-laminar shear strength parameters of the manufactured epoxy composites. The sample D-type has a greater strength property of 27.12 MPa among different kinds of manufactured epoxy hybrid materials, whereas the sample B-type has a lesser strength property of 20.36 MPa. It can be accomplished by including nanoscale SiO<sub>2</sub> fillers. The additional fillers were securely supported by PALF fibers,



© 2025. Advanced Journal of Engineering and Scientific Applications (AJESA) Vol. 2, No..1, 2025.

resulting in strong binding (Lakshmaiya et al. 2022). Inter-laminar shear force improved as the interaction among fillers and polymers improved. The presence of gaps and holes in the manufactured composites causes the hybrid composites to deteriorate faster, lowering the strength properties of the composites. The emergence of additional fractures and voids in B-type hybrids lowered inter-laminar shear capacity, and other researchers have seen comparable decreases ((Maurya et al. 2021); (Sormunen et al. 2019)).

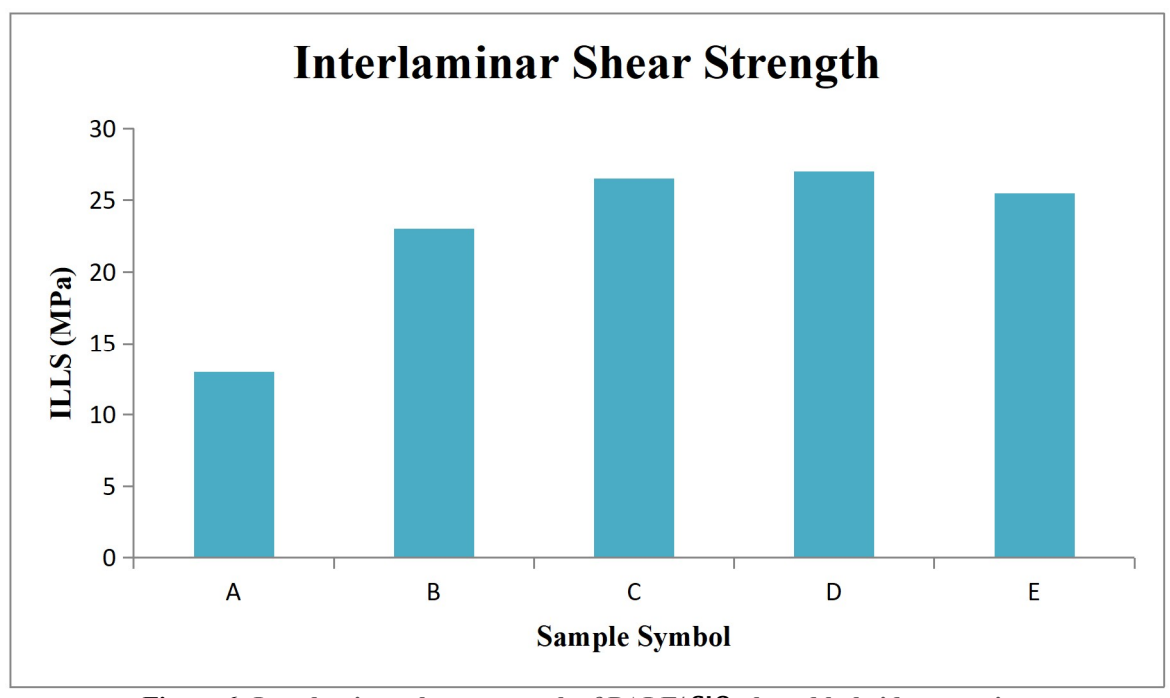


Figure 6: Interlaminar shear strength of PALF/SiO<sub>2</sub>-based hybrid composites

#### 3.2.4 Impact and Hardness Properties

An automated Izod impact tester was used to measure the fracture toughness of epoxy composite samples. Figure 7 depicts the fracture toughness of epoxy polymer hybrid composites as a function of the presence of SiO<sub>2</sub> nanoparticles. Figure 7 shows that the fracture toughness of the D and E-type composites has increased and reached the highest level of 6.32 and 5.24 kJ/m², respectively, which would be higher than the A, B, and C-type composites. The impact resistance of the polymer binder has also been determined to match the stiffness of the polymer system. The inclusion of 6% SiO<sub>2</sub> nanoparticles increased the stiffness of the epoxy-reinforced hybrid because SiO2 connects several different epoxy networks via -COOH and -OH structural features. Additionally, the inclusion of filler particles reduces the fracture toughness of the epoxy-reinforced hybrid by increasing the filler particle concentration (Sitticharoen et al. 2016). The fortification from pressing in the sample is referred to as the characteristic Shore D toughness. The shoreline D hardness values of the produced epoxy composite samples are shown in Figure 7. This specimen's Shore D toughness is mostly determined by stiffness. In this study, both the outer and interior sections of the SiO<sub>2</sub> sample were made of PALF fiber, and the SiO<sub>2</sub> nanoparticles became tougher. In comparison to hybrid composites, sample D does have the maximum value of Shore D toughness of 73.21, and similar findings were also investigated by Bharath et al. In comparison to hybrid composites, sample B (without filler) does have a smaller value of Shore D toughness at 41.36 owing to the decreased rigidity of PALF fabric.

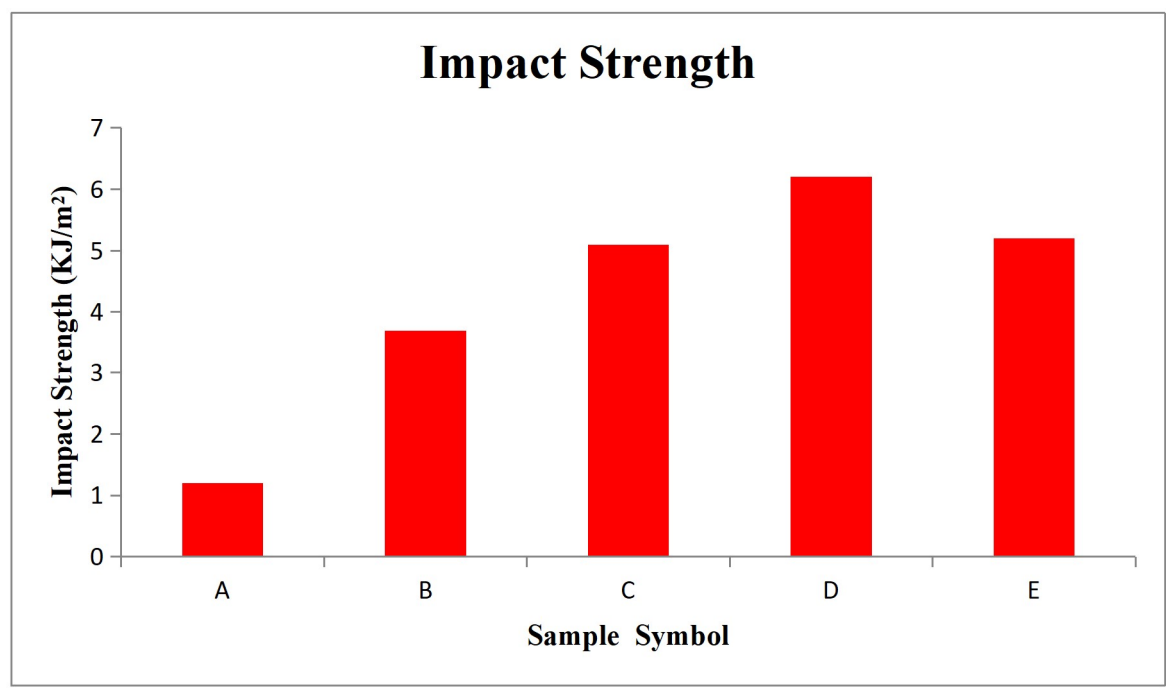


Figure 7(a): Impact strength of PALF/SiO<sub>2</sub>-based hybrid composites

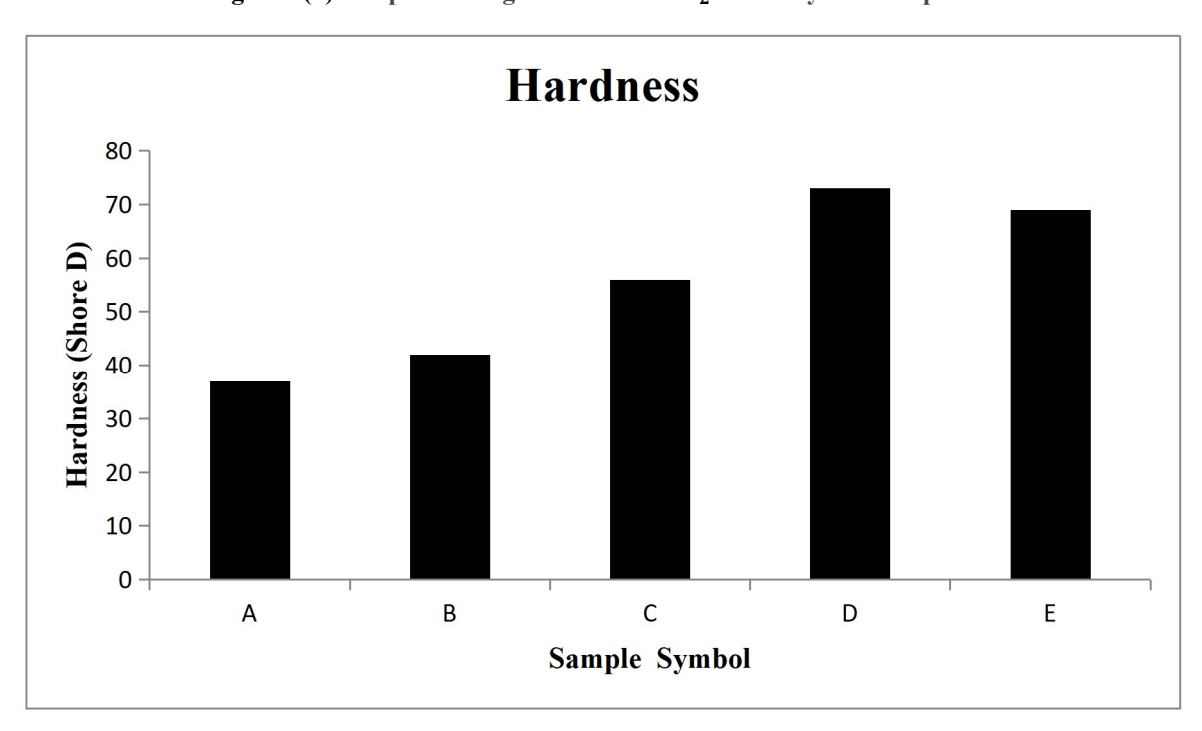


Figure 7(b): Hardness property of PALF/SiO<sub>2</sub>-based hybrid composites

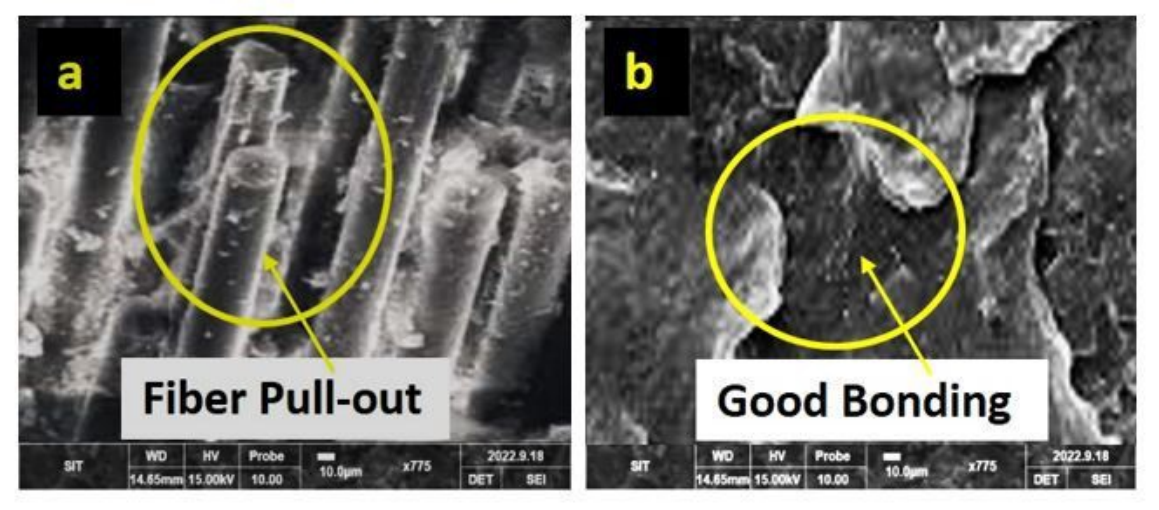
#### 3.2.5 Microstructural Analysis

The surface morphology of A, B, C, D, and E-type blends is shown in Figure 8. The PALF was strongly linked with the polymers in the PALF-reinforced epoxy (Figure 8(a)), as well as the rupture that developed throughout the fibers. This might be owing to the fundamental features of moisture absorption. Since PALF includes around 70% cellulose. Figure 8 (b) shows the SEM characterization of the composite's D type fractured tension reinforcement. PALF fibers and nanocrystalline SiO2 have been thoroughly entrenched in the epoxy, and the fibers have been coated and moistened with polymer. There aren't any visible cavities or gaps among the basic matrix and fiber. The direction of fibers within the matrices is crucial, as they seem to be dispersed equally at all four edges of the matrices (Natrayan et al. 2022). Effective binding at the intersection of PALF fiber, SiO<sub>2</sub>, and epoxy matrices results in excellent fiber and polymeric contact. The surface morphology was also found to be rough, with branching, bending cracking, and cracked locking. These properties were also investigated in the particulate epoxy sphere. The failure mode of the 9 wt. % SiO<sub>2</sub> and 25% PALF-reinforced epoxy polymers appeared coarse, and more particles appeared to have deboned



© 2025. Advanced Journal of Engineering and Scientific Applications (AJESA) Vol. 2, No..1, 2025.

from the polymers, as seen by the voids surrounding the fillers. Figure 8(c) also showed the existence of a basis for filler to accumulate. The concentration of SiO<sub>2</sub> nanoparticles acted as a carrier of failures, potentially reducing the material properties even more.



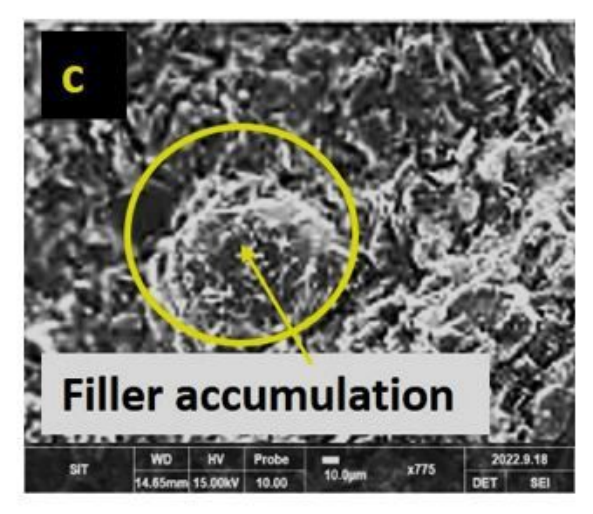


Figure 8: Micro-structural Images of (a) PALF, (b) PALF/6 wt. % of SiO<sub>2</sub>, (c) PALF/9 wt. % of SiO<sub>2</sub> -based hybrid composites

#### 3.3 Dynamic Mechanical Analysis

They are:

#### 3.3.1 Storage Modulus

Figure 9 illustrates the DMA curves of PALF materials and SiO<sub>2</sub>-based hybrid materials. Figure 9 also explains the storage modulus profiles of materials with a different weight proportion of SiO<sub>2</sub> filer. The maximum storage modulus at 30 °C is 6 wt. % SiO<sub>2</sub>/PALF. This seems to be owing to the composite's higher interfacial compliance, which limits the movement of polymeric chains and leads the contact between the fibers and the matrix to transfer greater loads, raising the rigidity of a material. The higher the loss ratio, the greater the amount of energy wasted by contact between the matrix and reinforcement.

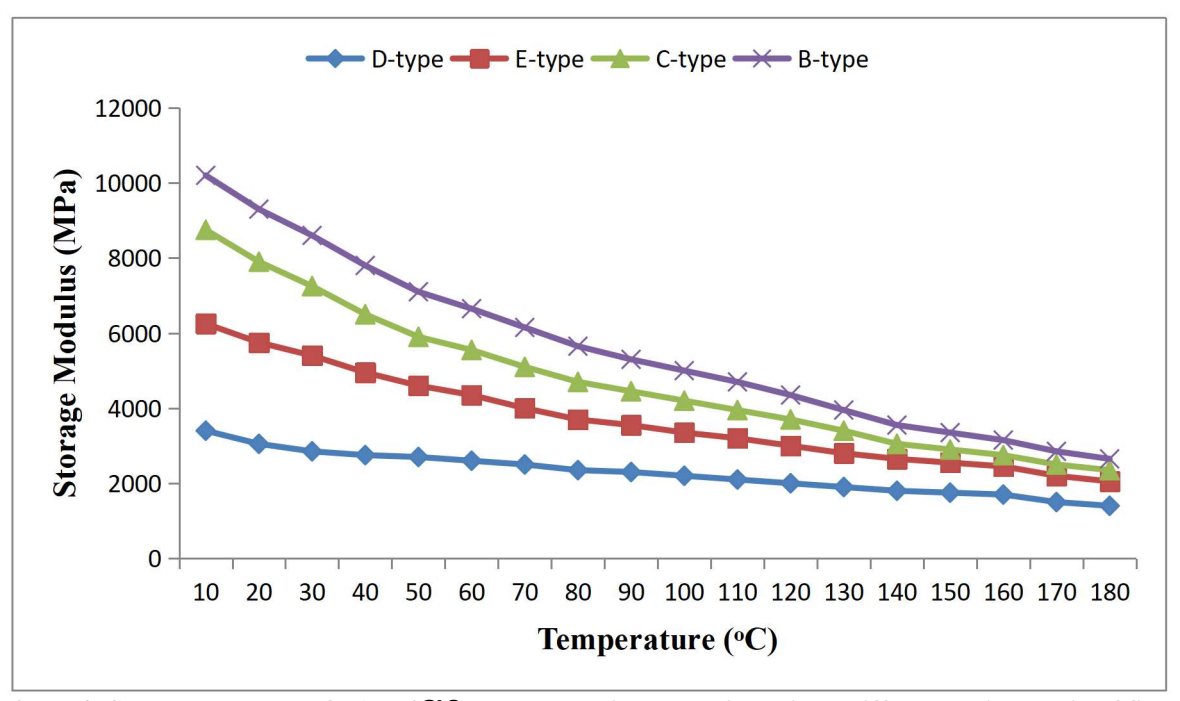


Figure 9. Storage Modulus of PALF/SiO<sub>2</sub>-based hybrid composites with a different weight ratio of filler content

#### 3.3.2 Loss Modulus

The proportion of loss modulus to storage modulus is equivalent to the value of the dissipation factor, which makes it an essential metric when evaluating the mechanical behavior of fiber-reinforced materials. Figure 10 depicts the tan curve of a mixture before and after alteration. The change in temperature graphs in the image demonstrates that the enhanced composite's temperature of glass transition (Tg) is generally rising. With a SiO<sub>2</sub> level of 6 wt. %, the Tg of a hybrid increases by 20°C to 156.6°C when compared to the PALF material. When the degree of polymerization changes from a glassy to a rubbery condition as the temperature increases, the polymer moves substantially higher cohesion and friction barriers, which leads to greater energy loss, a worse storage modulus, and increased failure. The contact of a SiO<sub>2</sub>/PALF composite with a weight of 6 % has a high adhesion property, a strong capacity to control the motion of an adhesive long sequence, as well as a low coecient of friction energy usage. As a result, its storage modulus diminishes rapidly, as does the amplitude of tan. Whenever the SiO<sub>2</sub> levels are excessive (9 wt%), aggregates on the fiber surface impede resin-fiber interaction, and interfacial bonding is poor, leading to greater energy dissipation (Chai et al. 2022).

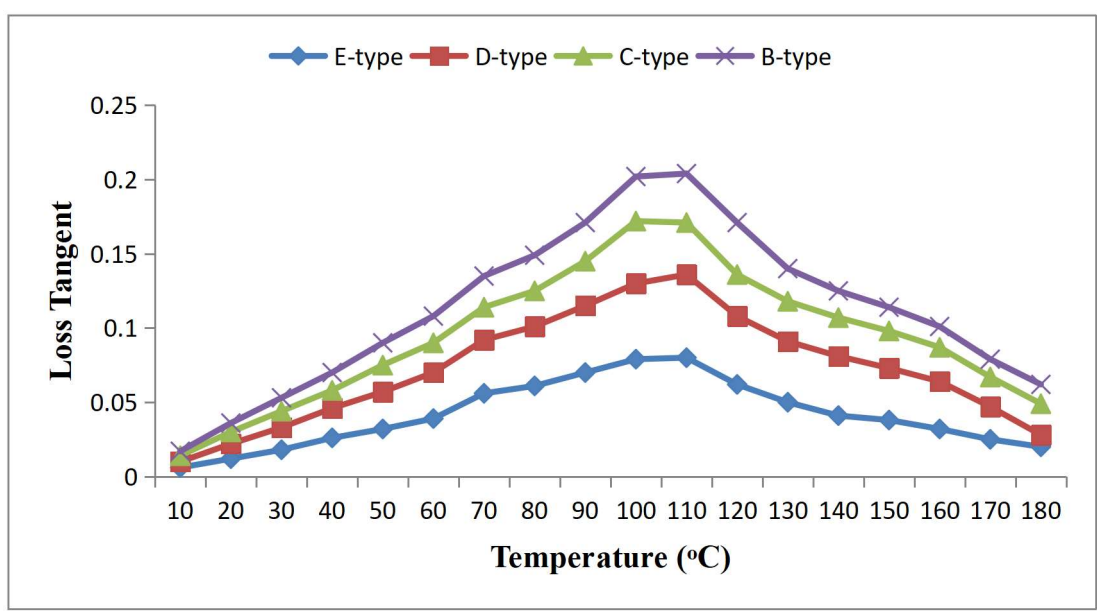


Figure 10. Loss Modulus of PALF/SiO2-based hybrid composites with a different weight ratio of filler content



© 2025. Advanced Journal of Engineering and Scientific Applications (AJESA) Vol. 2, No..1, 2025.

#### 3.4 Thermogravity Analysis

TGA is commonly used to assess the thermo-stability of materials. As seen in Figure 11, materials breakdown may be split into two phases: moisture and impurity breakdown (0 - 300 C), as well as resin condensation and degradation (300 – 600 °C). Because the mass decrease induced by moisture and impurity breakdown represents around 5 % of the overall mass, the temperatures equivalent to 95% of a starting weight are referred to as the original degradation temperature (Natrayan et al. 2022). Because the breakdown temperatures of PALF fiber and SiO<sub>2</sub> are substantially greater than 600°C, the decrease in quality materials beyond 400°C is entirely due to resin combustion and deterioration. Figure 11 reveals that the rst degradation rate of the SiO<sub>2</sub>-incorporated composites is nearly the same, at around 400°C, which is significantly higher than the starting decomposition temperature of PALF (300°C). This could indicate that the fiber and polymer get a stronger bond, which reduces the polymer's mobility and increases the mixture's thermo-stability. Also, the remaining weight of the composite changes drastically at 600°C. PALF, 3 wt. % SiO<sub>2</sub>, 6 wt.% SiO<sub>2</sub>, and 9 wt.% SiO<sub>2</sub> had residual masses of 60 %, 62 %, 56 %, and 50 %, respectively. Since the SiO<sub>2</sub> concentration is insufficient to be disregarded, we assume that the majority of the remaining section is made up of PALF fiber. The PALF fiber concentration in hybrids with 3 wt. % SiO<sub>2</sub> and 6 wt. % SiO<sub>2</sub> is lower compared to PALF. The possible explanation for this could be that the SiO<sub>2</sub> framework includes decreased interaction deficiencies, the closely packed framework between the ber and the epoxy allows the polymer to invade the fiber, the resin content is comparatively enhanced, as well as the fiber content is comparatively lowered, and the PALF fiber content is 9 wt.% SiO<sub>2</sub>, which might be attributable to aggregation on the fiber surface, but also precludes the efficient approach of fiber and matrix, culminating in so many deficiencies and holes in the specimen.

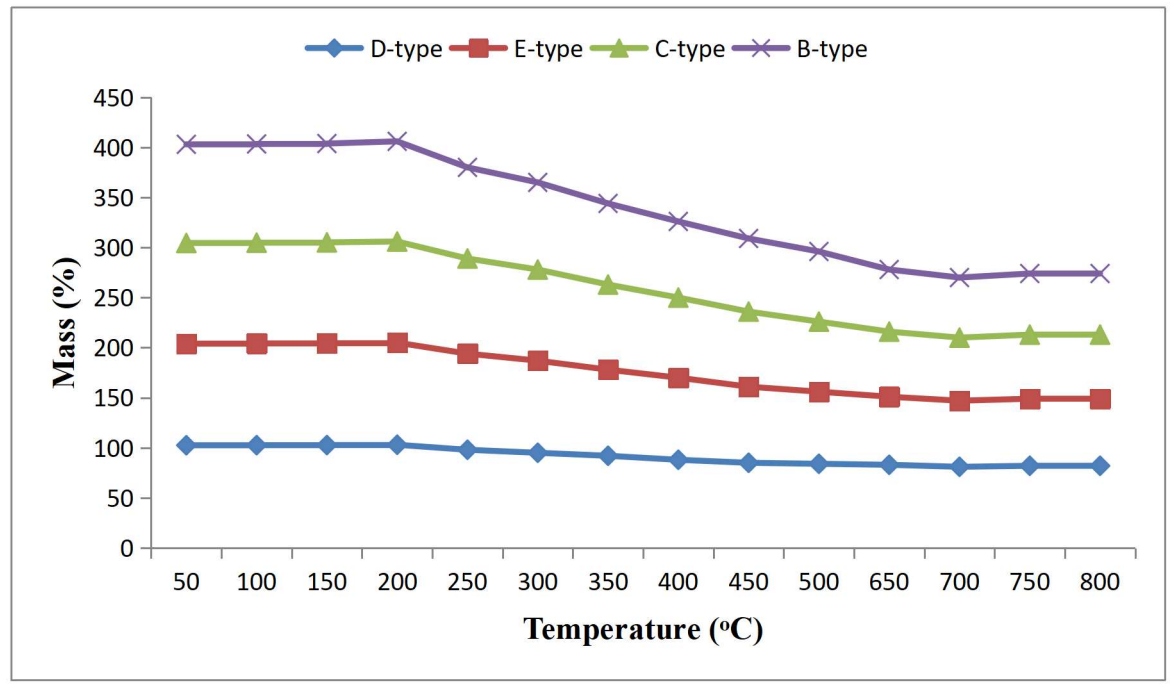


Figure 11. Storage Modulus of PALF/SiO<sub>2</sub>-based hybrid composites with a different weight ratio of filler content

#### 3.4 Moisture Absorption Behaviour

Figure 12 depicts the water absorption properties of PALF and PALF/ SiO<sub>2</sub> polymer composites. It is mostly determined by Fickian diffusion. Moisture content is critical for all living things. It also becomes absorbed after 60 days. For all epoxy composite samples, both the maximal water usage and the beginning time for moisture absorption increased. Water uptake qualities of composite resin are examined using factors such as immersion time, filler-to-polymer ratio, processing technologies, filler, and matrix characteristics in a given environmental condition. The hydrophilic properties of leaf fibers are mainly accountable for this moisture absorption. Moisture is mostly utilized by the additives found in polymer composites strengthened with lignocellulosic biomass, such as PALF. Because the epoxy resin is hydrophobic, its moisture consumption may be decreased. Likewise, the water uptake behavior of SiO<sub>2</sub> nanoparticle-loaded PALF epoxy hybrid lamination is lower than that of PALF hybrids. The SiO<sub>2</sub> nanocrystals reduce the vacancy fraction of the composites, resulting in a reduction in water uptake capacity (Velmurugan et al. 2022). Moisture resilience is improved in the altered composites.

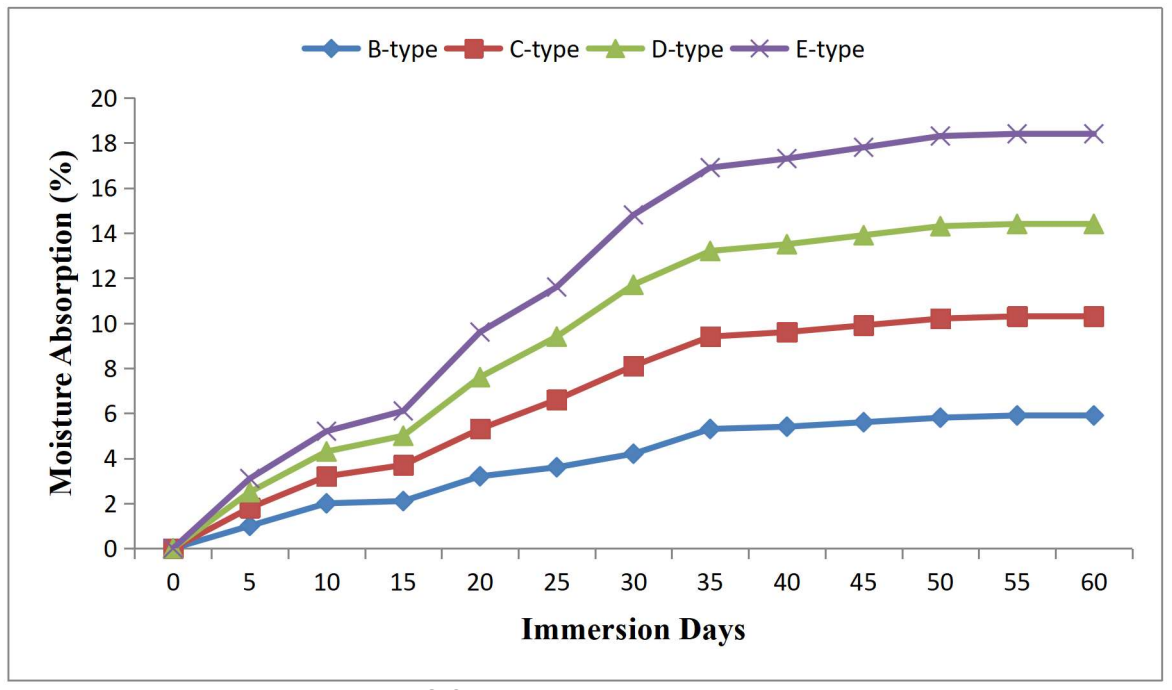


Figure 12. Storage Modulus of PALF/ SiO<sub>2</sub>-based hybrid composites with a different weight ratio of filler content

#### 4. CONCLUSION

PALF fiber reinforced with varied weight proportions of SiO<sub>2</sub> filler-based hybrid composites were generated in this experiment, and the composites were tested for mechanical characteristics such as tensile, bending, hardness, ILSS, impact strength, and dynamic mechanical analysis. The following conclusions were drawn from the findings: The bending vibration of N-H groupings around 2800 cm<sup>-1</sup> was widened, perhaps due to interactions of hydrogen bonds among SiO<sub>2</sub> nanoparticles and PALF fiber. Trend shifts from 1793 to 1798 cm<sup>-1</sup> as well as 3640 to 3680 cm<sup>-1</sup>, correspondingly, guarantee the presence of the hydroxyl group among-OH and -C = O. The vibrating wavelength of Si-OH changes from 3923 to 3969 cm-1, indicating the presence of silicon in the epoxy. Among the five different types of composites i.e A, B, C, D and E types, the D-type composite (25 wt.% of PALF with 6 wt.% of SiO<sub>2</sub> filler) reveals high tensile (46.18 MPa) and E-type (25 wt.% with 9 wt.% SiO<sub>2</sub>) composites reveals high flexural (58.96 MPa) strength. Even though contrasted with pure resin, hybrids laminate C, D, and E-type demonstrated 13.25 %, 23.36%, and 20.36% increases in tensile strength as well as 32.65 %, 45.62 %, and 4012 % increases in elastic strength. The flexural strengths rose by 30 %, 42 %, and 45 % in bio-composites such as C-type, D-type, and E type, respectively. This increase was caused by the efficient load transfer across matrices to reinforcements as a consequence of the strong esters, hydroxyls, and nylon binding interactions among PALF fiber and resin, as well as the good distribution of nanocrystalline silicon dioxide. The sample D-type has a greater ILSS property of 27.12 MPa among different kinds of manufactured epoxy hybrid materials, whereas the sample B-type has a lesser strength property of 20.36 MPa. Inter-laminar shear force improved as the interaction among fillers and polymers improved. According to the SEM analysis the failure mode of the 9 wt. % SiO<sub>2</sub> and 25 % PALF-reinforced epoxy polymers appeared coarse, and more particles appeared to have deboned from the polymers, as seen by the voids surrounding the fillers. According to TGA results the rst degradation rate of the SiO<sub>2</sub>-incorporated composites is nearly the same, at around 400°C, which is significantly higher than the starting decomposition temperature of PALF (300°C). This could indicate that the ber and polymer get a stronger bond, which reduces the polymer's mobility and increases the mixture's thermostability. The water uptake behavior of SiO<sub>2</sub> nanoparticle-loaded PALF epoxy hybrid lamination is lower than that of PALF hybrids. Declarations Authors' contributions Velmurugan G: Conceptualization, Writing an original draft, Methodology.

#### **Conflict of interest**

The authors declare that there is no conflicting interest in the publication of this paper.

#### Acknowledgements

This paper was not supported by any financial grant from granting bodies. The authors really appreciate by acknowledging Engr. Dr. George. O. O. for his active inputs and contributions needed for the outcome of this publication financially and otherwise.



© 2025. Advanced Journal of Engineering and Scientific Applications (AJESA) Vol. 2, No..1, 2025.

#### References

- Gholampour, A., Ozbakkaloglu, T. (2020). A review of natural fiber composites: properties, modification and processing techniques, characterization, applications. Springer US
- Väisänen, T., Das, O., Tomppo, L. (2017). A review on new bio-based constituents for natural fiber polymer composites. Journal of Cleaner Production 149:582–596. https://doi.org/10.1016/j.jclepro.2017.02.132
- Velmurugan, G., Babu, K. (2020). Statistical analysis of mechanical properties of wood dust filled Jute fiber based hybrid composites under cryogenic atmosphere using Grey-Taguchi method. Materials Research Express 7:. https://doi.org/10.1088/2053-1591/ab9ce9
- Sharma, M., Sharma, R., Chandra Sharma, S. (2020). A review on fibres and fillers on improving the mechanical behaviour of fibre reinforced polymer composites. Materials Today: Proceedings 46:6482–6489. https://doi.org/10.1016/j.matpr.2021.03.667.
- Gouda, K., Bhowmik, S., Das, B. (2021). A review on allotropes of carbon and natural filler-reinforced thermomechanical properties of upgraded epoxy hybrid composite. Reviews on Advanced Materials Science 60:237–275. https://doi.org/10.1515/rams-2021-0024
- Sanjay, M. R., Madhu, P., Jawaid, M. (2018). Characterization and properties of natural fiber polymer composites: A comprehensive review. Elsevier B.V.
- Johny, V., Kuriakose Mani, A., Palanisamy, S. (2023). Extraction and Physico-Chemical Characterization of Pineapple Crown Leaf Fibers (PCLF). Fibers 11:5. https://doi.org/10.3390/ b11010005
- Todkar, S. S., Patil, S. A. (2019). Review on mechanical properties evaluation of pineapple leaf bre (PALF) reinforced polymer composites. Composites Part B: Engineering 174:106927. https://doi.org/10.1016/j.compositesb.2019.106927
- G V, K B, L IF .(2020). Optimization on Mechanical Behavior of Hemp and Coconut Shell Powder Reinforced Epoxy Composites Under Cryogenic Environment Using Grey-Taguchi Method. SSRN Electronic Journal. https://doi.org/10.2139/ssrn.3654034
- Velmurugan, G., Siva Shankar, V., Kalil Rahiman, M. (2023). Effectiveness of silica addition on the mechanical properties of jute/polyester based natural composite. Materials Today: Proceedings 72:2075–2081. https://doi.org/10.1016/j.matpr.2022.08.138
- Tang, C., Li, X., Yin, F., Hao, J. (2017). The performance improvement of aramid insulation paper by nano SiO<sub>2</sub> modification. IEEE Transactions on Dielectrics and Electrical Insulation 24:2400–2409. https://doi.org/10.1109/TDEI.2017.006560
- Ponnusamy, M., Natrayan, L., Patil, P. P. (2022). Multiresponse Optimization of Mechanical Behaviour of Calotropis gigantea/Nano-Silicon-Based Hybrid Nanocomposites under Cryogenic Environment. Adsorption Science and Technology. https://doi.org/10.1155/2022/4138179
- Chai, R., Zhu, W., Li, Q. (2022). Effect of Basalt Fiber Content on Mechanical and Tribological Properties of Copper-Matrix Composites. Metals 12:. https://doi.org/10.3390/met12111925
- Kavya, H. M., Bavan, S., Yogesha, B. (2021). Effect of coir fiber and inorganic filler on physical and mechanical properties of epoxy based hybrid composites. Polymer Composites 42:3911–3921. https://doi.org/10.1002/pc.26103
- Hoque, M. B., Hossain, M. S., Nahid, A. M. (2018). Fabrication and Characterization of Pineapple Fiber Reinforced Polypropylene Based Composites. Nano Hybrids and Composites 21:31–42. https://doi.org/10.4028/www.scientic.net/nhc.21.31
- Natrayan, L., Kumar, P. V. A., Baskara Sethupathy, S. (2022). Water Retention Behaviour and Fracture Toughness of Coir/Pineapple Leaf Fibre with Addition of Al<sub>2</sub>O<sub>3</sub> Hybrid Composites under Ambient Conditions. Adsorption Science and Technology 2022:. https://doi.org/10.1155/2022/7209761



- Hamid, N. H., Hisan, W. S. I.W. B., Abdullah, U. H. (2019). Mechanical properties and moisture absorption of epoxy composites mixed with amorphous and crystalline silica from rice husk. BioResources 14:7363–7374. https://doi.org/10.15376/biores.14.3.7363-7374
- Lakshmaiya, N., Ganesan, V., Paramasivam, P., Dhanasekaran, S. (2022). Influence of Biosynthesized Nanoparticles Addition and Fibre Content on the Mechanical and Moisture Absorption Behaviour of Natural Fibre Composite. Applied Sciences (Switzerland) 12:.https://doi.org/10.3390/app122413030
- Maurya, A. K., Gogoi, R., Manik, G. (2021). Mechano-chemically activated y-ash and sisal fiber reinforced PP hybrid composite with enhanced mechanical properties. Cellulose 28:8493–8508. https://doi.org/10.1007/s10570-021-03995-4
- Sormunen, P., Kärki, T. (2019). Recycled construction and demolition waste as a possible source of materials for composite manufacturing. Journal of Building Engineering 24:100742. https://doi.org/10.1016/j.jobe.2019.100742
- Sitticharoen, W., Chainawakul, A., Sangkas, T., Kuntham, Y. (2016). Rheological and mechanical properties of silicabased bagasse-fiber-ash-reinforced recycled HDPE composites. Mechanics of Composite Materials 52:421–432. https://doi.org/10.1007/s11029-016-9594-z
- Natrayan, L., Kumarm, P. V. A., Baskara Sethupathy, S. (2022). Effect of Nano TiO2Filler Addition on Mechanical Properties of Bamboo/Polyester Hybrid Composites and Parameters Optimized Using Grey Taguchi Method. Adsorption Science and Technology. https://doi.org/10.1155/2022/6768900
- Natrayan, L., Kumar, P. V.A., Kaliappan, S. (2022). Optimisation of Graphene Nano filler Addition on the Mechanical and Adsorption Properties of Woven Banana/Polyester Hybrid Nanocomposites by Grey-Taguchi Method. Adsorption Science and Technology. https://doi.org/10.1155/2022/1856828
- Velmurugan, G., Siva Shankar, V., Natrayan, L. (2022). Multi-response Optimization of Mechanical and Physical Adsorption Properties of Activated Natural Fibers Hybrid Composites. Adsorption Science & Technology, 1–16. https://doi.org/10.1155/2022/1384738
- George O. Okoronkwo, Kizito Chidozie Ibe, Simeon I. Bright. (2022). Application of ANN and RSM on the strength properties of alkali mercerized hybrid ramie-isora fibre reinforced biodegradable composites, *Journal of Inventive Engineering and Technology* (JIET), A Publication of the Nigerian Society of Engineers, Awka Branch. Vol. 2, Issue 3, pp. 40-61. @ Nigerian Society of Engineers, Awka Branch.
- Ezeokpube Greg C., Okoronkwo George O, Onodagu Peter D. (2021). Natural fiber reggressors effects on physical and strength properties responses of bidirectional finger root fiber reinforced epoxy composites, *Journal of Inventive Engineering and Technology* (JIET), A Publication of the Nigerian Society of Engineers, Awka Branch. Vol. 1, Issue 5, pp. 1-15. @ Nigerian Society of Engineers, Awka Branch.

Ezeokpube Greg C., Okoronkwo George O, Onodagu Peter D. (2021). Strength properties analysis of biomimetic natural wire weed fiber reinforced polymer composite honeycomb plates, *Journal of Inventive Engineering* and *Technology* (JIET), A Publication of the Nigerian Society of Engineers, Awka Branch, Vol. 1, Issue 5, pp. 16-28.

@ Nigerian Society of Engineers, Awka Branch.